Signal, Image and Video Processing (2025) 19:26
https://doi.org/10.1007/s11760-024-03655-7

ORIGINAL PAPER

Feature integration for frontal gait recognition through contour image analysis

R. Anusha[1] · **C. K. Sunil**[2]

Received: 4 April 2024 / Revised: 27 September 2024 / Accepted: 2 October 2024

Abstract
Biometric technology is advancing with gait recognition, which analyzes walking patterns to identify people. This pattern is derived without the direct participation of individuals, from a distance. Frontal gait data is highly valuable in confined spaces like narrow corridors, which is common in most buildings. Within this scope, this study introduces a successful approach to identify individuals in frontal-view gait sequences. By utilizing contour image and vertices, the proposed method obtains three differentiating feature vectors from the Gait Energy Image (GEI). Its efficient capture of spatial dynamics leads to improved gait recognition performance. The proposed approach's effectiveness was evaluated using the widely used gait datasets such as CMU MoBo, CASIA A, and CASIA B. Through the experiments, it was proven that the proposed approach delivers promising outcomes and performs better than certain state-of-the-art approaches in recognition.

Keywords Gait energy image · Gait recognition · Feature extraction · Classification

1 Introduction

The biometric recognition system has become an integral part of numerous real-world applications, given its compelling nature. Fingerprint, face, and iris recognition are among the biometric systems that have gained significance and reliability in real-world applications. The way someone walks, known as gait, is also considered a biometric trait. The reason why gait recognition is appealing is because it can identify individuals by analysing their walking mannerisms, even from a distance. Concealing one's gait is challenging. Unlike other behavioural biometric traits, this one can be evaluated without any physical interaction. Therefore, Its significance in surveillance applications is evident [1, 2].

In general, gait detection approaches can be categorized as either appearance-based or model-based. The model-based methods in use gait sequences to model the motion of the human body [3]. These techniques analyse joint movements in order to measure various aspects of gait, including direction, hip, knee, ankle, and hand movements. These methodologies are not only scale invariant, they are also computationally expensive since they require the modelling and tracking of the subject's body. In addition, high-resolution images are also required by them. On the flip side, appearance-based methods involve performing operations directly on gait silhouette images, bypassing the use of an explicit model. According to recent literature, the use of different templates in appearance-based approaches has yielded highly successful outcomes in gait identification.

The following part focuses solely on frontal gait recognition research. Soriano et al. [4] developed a descriptor called curve spread specifically for front view gait videos. Using Freeman code, the time-variations of a moving body's outline are represented as a 2D vector. Further, the feature extraction method proposed by Anusha and Jaidhar is based on shape descriptor. To classify frontal gait silhouettes, they employed a method called similarity measurement. The authors Sivapalan et al. [5] put forth a recommendation for a method using frontal depth images. Here, the GEl concept is expanded to 3D, leading to the development of gait energy volume. Additionally, the study highlights the effectiveness of recon-

✉ R. Anusha
anur.research@gmail.com

C. K. Sunil
sunilck@iiitdwd.ac.in

[1] Department of Computer Science and Engineering, Bapuji Institute of Engineering and Technology, Davanagere, Karnataka 577004, India

[2] Department of Computer Science and Engineering, Indian Institute of Information Technology Dharwad, Dharwad, Karnataka 580009, India

Published online: 02 December 2024

structing partial volumes using depth images from the front view.

The solution presented by Chattopadhyay et al. [6] for occlusion in frontal gait recognition involves the use of kinetic depth data. They extract features from the depth data and silhouette edge to capture the back view. The authors Chattopadhyay et al. [7] developed the feature pose depth volume by reconstructing the surface's partial volume from frontal view silhouettes. The author also suggested a hierarchical classification strategy that combines the descriptors from RGB-D cameras [8]. A gait template known as "marching in place" was proposed by Ryu and Kamata [9] to maintain the spatial and temporal features of human gait sequences. Most of these methods employ frontal gait recognition, but they typically rely on gait data from Kinect with a limited number of subjects for performance analysis.

Maity et al. [10]'s study addresses two important issues that have been overlooked in surveillance video research. Here, the robust gait recognition framework is achieved using only the frontal view images by combining model-free and model-based gait feature extraction. Moreover, it makes use of a low-resolution face recognition approach that can be trained and tested with low-resolution facial characteristics. Deng et al. [11] presents a new approach to gait recognition, focusing on frontal views and incorporating gait dynamics and deep learning. The author examines binary walking silhouettes in this work by analysing three frontal-view gait features: spatial ratio, kinematic, and area. Zhang et al. [12] introduces GaitNet, a groundbreaking framework that extracts canonical, appearance, and pose features from RGB images. The LSTM captures dynamic gait features by integrating pose features over time and uses canonical features for static gait representation. The relationship between silhouette and dense optical flow features in frontal gait images was investigated by Deng et al. [13] using the multi-modal fusion module, squeeze and excitation operations.

Sheshadri and Okade [14] examines how Kinect can be used for gait recognition of individuals in surveillance settings, particularly in narrow corridors and airports where only frontal views are accessible. A hierarchical framework is created to identify the subject that closely matches by incorporating two skeleton features and one feature obtained from segmenting depth data. Deng et al. [15] proposes an innovative approach to identify human gait by utilizing gait dynamics and deep transfer learning. The frontal human silhouettes in this work are characterized by four gait features that undergo changes over time: lower limb area ratio, lower limb length ratio, swing angle of lower limb, and swing area of lower limb. In conclusion, It can be inferred that the majority of recent research in frontal gait recognition depends on spatial data for enhanced recognition performance.

2 Motivation and contributions

Despite significant advancements in gait recognition, system performance is primarily influenced by various covariate factors including walking speed, view angle changes, elapsed time, walking surface, and carrying conditions. Among the different covariates, the variations in view angle stand out as a crucial factor. In the frontal view, the spatial and temporal differences in the gait data are less noticeable than in other views. [15–17]. This study presents an approach that improves the effectiveness of the frontal gait recognition system.

Based on the above discussion in introduction, appearance based methods are not only superior to model-based methods in terms of performance, but also more suitable for surveillance environments and computationally efficient [2, 18–20]. Gait features are derived by extracting shapes and contours from human silhouette images in most appearance-based individual identification systems.

Pattern recognition, image analysis, and computer vision methods rely heavily on contour detection as a primary step. Utilizing a contour detection algorithm on a gait image produces connected vertices and curves that indicate subject boundaries and surface orientation discontinuities. By applying the contour detection algorithm to a gait image, there can be a substantial decrease in the amount of information that needs to be processed. Additionally, it has the potential to discard less important data while preserving the main structural features of a gait image. Thus, this paper introduces a gait representation method that utilizes spatial features extracted from GEI's contour image and vertices.

To sum up, this study's contributions are as follows:

1. This study introduces three feature vectors that improve the reliability and provide a more accurate representation of the spatial variations in a frontal gait.
2. The feature vectors being proposed comprise of features from the frontal contour image that are uniformly distributed and track small alterations in the GEI shape. This leads to an improvement in gait recognition performance as the inter-class variance increases.
3. Utilizing both ensemble classifier and feature modeling together, the proposed system achieves better results.
4. Performance evaluation of the proposed method involved a comprehensive experiment using widely used gait datasets. The results are evaluated in relation to state-of-the-art and other contour-based gait recognition techniques.

The proposed method specifically handles frontal gait, which has multiple uses like a classroom attendance system that captures student data upon entering a classroom from front view. The same can be applied to employees in any

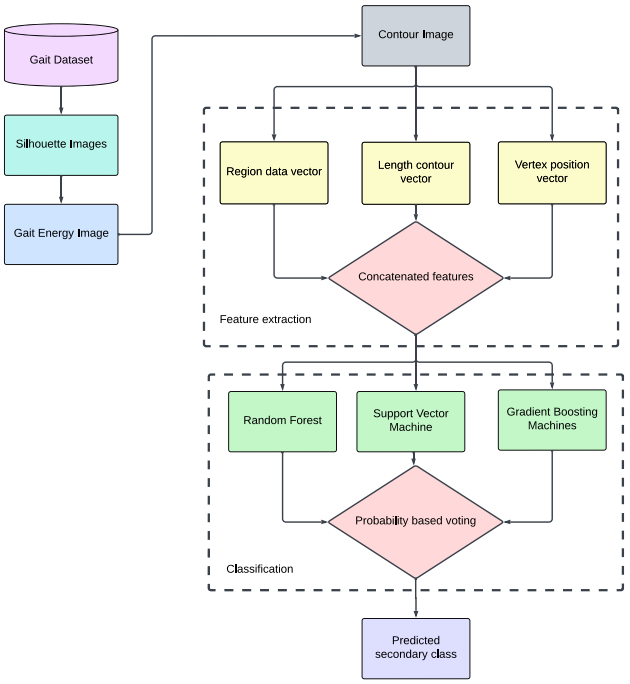

Fig. 1 The proposed framework for gait recognition

organization, capturing their data as they enter. This monitors or gathers information about people walking in a building. This can also function as a means of access control, preventing certain individuals from entering a space. That refers to the prevention of unauthorized access to certain areas. Generally, in wide spaces, recognition can be accomplished by using the side view. In situations like narrow corridors where space is limited, frontal data is extremely valuable, and this is often the case in most buildings. Frontal images have an abundance of spatial data, but lack significant temporal or dynamic data. Further, the utilization of contour images and vertices in Gait Energy Images allows for the effective extraction of distinctive features, leading to a higher recognition accuracy as spatial data dominates frontal images.

Further, section 3 of the paper offers a detailed explanation of the proposed methodology, while Sect. 4 presents an illustration of the experimental results. The conclusions are provided in Sect. 5.

3 Proposed method

Figure 1 illustrates the outline of the proposed method. It is composed of three different stages. The gait silhouettes are merged to create a GEI during the initial stage. The GEI is used to extract the contour vertices and contour image. During the second stage, the contour vertices and contour image of the subjects in both the training and testing dataset produce three distinct feature vectors. At last, the features are classified by the proposed ensemble classifier. The testing dataset is used to measure the performance of the gait recognition system, which is indicated by the Correct Classification Rate (CCR).

3.1 Extraction of contour image and vertices

The GEI maintains and portrays the fluctuations in a gait pattern's spatial and temporal aspects. Compared to the other lateral views, the temporal information present in frontal view GEI template is minimal. Hence, developing a compact representation for spatial data can enhance the performance of frontal gait recognition by increasing inter-class variance. So, extracting the contour of the GEI allows for obtaining precise shape details, facilitating the accomplishment of this task.

To create a contour for a GEI image, the marching squares algorithm [21] is utilized with an isovalue of 0.5, and the precise contour position is determined through linear interpolation. When this method is used on the GEI, it generates a collection of vertices $S(x, y)$. The GEI's boundary is defined by these vertices. Therefore, it demonstrates that the GEI front view has limited temporal information. Figure 2 illustrates the use of these vertices to obtain a greyscale contour image, $GCI(x, y)$.

3.2 Feature extraction

Increasing the performance of a gait recognition system is highly dependent on extracting the most discriminatory feature vectors. The steps of feature extraction are demonstrated in Algorithm 1.

Here is the mention and explanation of the three proposed feature vectors: (1) Region data vector, (2) Length contour vector, and (3) Vertex position vector.

Algorithm 1 Feature extraction

Input: GCI, of size $p \times q$.
Output: Feature vector, FV.
Process an input contour image.
Calculate the region data vector, RD_v.
Compute length contour vector, L_C.
Compute vertex position vector, Ver_v.
The three feature vectors are concatenated to form the final feature vector, $FV = \{RD_v, L_C, Ver_v\}$

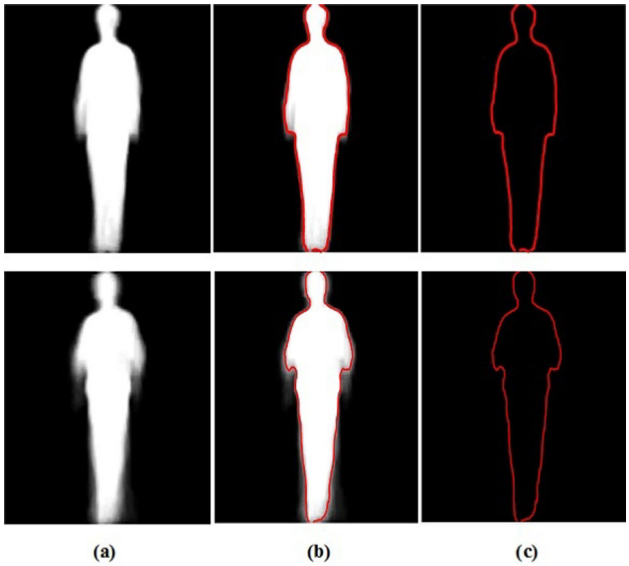

Fig. 2 The CASIA B gait dataset sample images of two subjects, showcasing **a** GEI, **b** a contour generated through marching squares algorithm and linear interpolation, and **c** a contour image

3.3 Region data vector

Let's take into account a greyscale contour image (GCI) that has a size of $p \times q$.

$$GCI = \begin{bmatrix} GCI_{(1,1)} & GCI_{(1,2)} & ..... & GCI_{(1,q)} \\ GCI_{(2,1)} & GCI_{(2,2)} & ..... & GCI_{(2,q)} \\ . & . & ..... & . \\ . & . & ..... & . \\ GCI_{(p,1)} & GCI_{(p,2)} & ..... & GCI_{(p,q)} \end{bmatrix} \quad (1)$$

The rows of the GCI are represented by $rw_1, rw_2, ..., rw_p$ and the columns are represented by $cn_1, cn_2, ..., cn_q$. All pixels outside the contour in the GCI that have an intensity value of 0 should be replaced with 255. The contour replacement results in the shape of the subject being represented by the pixels with intensity 0 in the GCI.

3.3.1 Horizontal span

The number of 0 intensity pixels in each row of the contour image is used to compute the horizontal span. Suppose we have a contour image, $GCIh$, and let rw_k denote the k^{th} row within it.

Here, rw_k= $[GCIh_{(k,1)}\, GCIh_{(k,2)} \ldots GCIh_{(k,q)}]$. In this instance, the value of a pixel at position $GCIh_{(k,j)}$, where $j = 1, 2, .., q$, is provided by

$$GCIh_{(k,j)} = \begin{cases} 1 & \text{if } GCIh_{(k,j)} = 0 \\ 0 & otherwise \end{cases} \quad (2)$$

The row rw_k has a horizontal span of rw_k, which is calculated as the sum of $GCIh_{(k,j)}$ for all j from 1 to q. That is, $rw_k = \sum_{j=1}^{q} GCIh_{(k,j)}$

3.3.2 Vertical span

The number of pixels with intensity value 0 in each column of the contour image is counted to calculate the vertical span followed by keeping a count column-wise. Consider a contour image, $GCIv$ and let rc_k be the k^{th} column in $GCIv$.

$$rc_k = \begin{bmatrix} GCIv_{(1,k)} \\ GCIv_{(2,k)} \\ . \\ . \\ GCIv_{(p,k)} \end{bmatrix} \quad (3)$$

The value of a pixel at position $GCIv_{(z,k)}$, where $z = 1, 2, ..., p$, can be determined using this equation.

$$GCIv_{(z,k)} = \begin{cases} 1 & \text{if } GCIv_{(z,k)} = 0 \\ 0 & otherwise \end{cases} \quad (4)$$

The column rc_k has a vertical span of vc_k, which is calculated as the sum of $GCIv_{(z,k)}$ for z ranging from 1 to p.

Consider the horizontal span obtained by removing values equal to 0, labeled as GCH_w=$[hr_1\, hr_2 \ldots hr_p]$ of size $1 \times p$. Also, let $GCV_l = [vc_1\, vc_2 \ldots vc_q]$ be the vertical span obtained for the after removing the values with vc_k equals to 0.

Concatenate the horizontal span vector GCH_w with the vertical span vector GCV_l in order to obtain the region vector RD_v. Take the RD_v vector and divide each of its elements by the total number of elements, t.

$$RD_v = \left[rd_1/t\ rd_2/t\ .....\ rd_t/t\right] \quad (5)$$

When dealing with fuzzy sets, the information value is calculated by multiplying the information source value with its Membership Function (MF) value [22]. By utilizing the information set, which is a collection of these values, we can extract spatial dynamics as depicted below.

The source of information being considered is the region vector denoted as:

$$RD_v = \left[RD_1 \ \ldots\ RD_t\right] \quad (6)$$

In order to calculate Gaussian MF, we obtain the mean and standard deviation by:

$$\mu^{RD} = \frac{1}{t}\sum_{i=1}^{t} RD_i \quad \text{and} \quad \sigma^{RD} = \frac{1}{t}\sum_{i=1}^{t}(RD_i - \mu^{RD})^2 \quad (7)$$

The following gain function is utilized to obtain the vector of Gaussian MF.

$$g(RD_i) = e^{-(RD_i - \mu^{RD}/\sigma^{RD})^2} \quad \text{where} \quad i = 1, 2..., t. \tag{8}$$

The region data vector is derived by extracting the features of the region vector. That is,

$$RD_v = \left[RD_1 \times g(RD_1) \ \ldots \ RD_t \times g(RD_t)\right] \tag{9}$$

3.4 Length contour vector

Representing the contour's vertices as $C(x_d, y_d)$, we have d ranging from 1 to n. There are three distance algorithms that can be used to calculate the distance between two consecutive vertices $C(x_m, y_m)$ and $V(x_{m+1}, y_{m+1})$.

The length of the contour vector is determined by adding the distances between consecutive vertices, (R_L). That is, Euclidean: $EUC_m = \sqrt{(x_m - x_{m+1})^2 + (y_m - y_{m+1})^2}$, the next is, Manhattan : $MAN_m = |x_m - x_{m+1}| + |y_m - y_{m+1}|$, and
Chebyshev : $CHE_m = max\{|x_m - x_{m+1}|, |y_m - y_{m+1}|\}$.

The sum of distances between consecutive vertices gives the contour length vector (L_C). It is provided by:

$$L_C EUC = EUC_1 + EUC_2 + ... + EUC_{n-1} \tag{10}$$
$$L_C MAN = MAN_1 + MAN_2 + ... + MAN_{n-1} \tag{11}$$
$$L_C CHE = CHE_1 + CHE_2 + ... + CHE_{n-1} \tag{12}$$

3.5 Vertex position vector

This vector aims to extract the positional information of every contour vertex. Consider a GCI of size $m \times n$, where the value of m and n is equal. Divide it into two equal contours. that is, right and left contour. Denote the vertex on the right and left contour as $Ver_L(x, y)$ and $Ver_R(x, y)$. The next step is to calculate the arctangent for the specified x and y coordinates of vertex $Ver_L(x, y)$ and $Ver_R(x, y)$. The arctangent of any vertex $Ver(x, y)$ is expressed as $Ver_\theta = atan2(x, y)$.

Extracting the arctangent of all contour vertices (left and right contour) results in the formation of the vertex position vector, which contains the location information. The formation of a vertex position vector is indicated by:

$$Ver_v = \left[Ver_{\theta 1} \ Ver_{\theta 2} \ \ldots \ Ver_{\theta n-1} \ Ver_{\theta n}\right] \tag{13}$$

3.6 Feature representation

The discriminative ability of the extracted feature vector is shown in the four feature space diagrams. The features derived from the horizontal span and vertical span vector are illustrated in Fig. 3 and 4. The features from the length contour vector are illustrated in Fig. 5. Figure (3), (4), and (5) illustrate the feature vectors extracted from different CI's (Contour Image) and subjects, with the first diagram (a) showing three CI's of the same subject and the second diagram (b) displaying features from a single CI of three different subjects. The feature space diagram clearly indicates that there are minimal variations within three gait cycles for the same subject, but significant variations between the gait cycles of three different subjects.

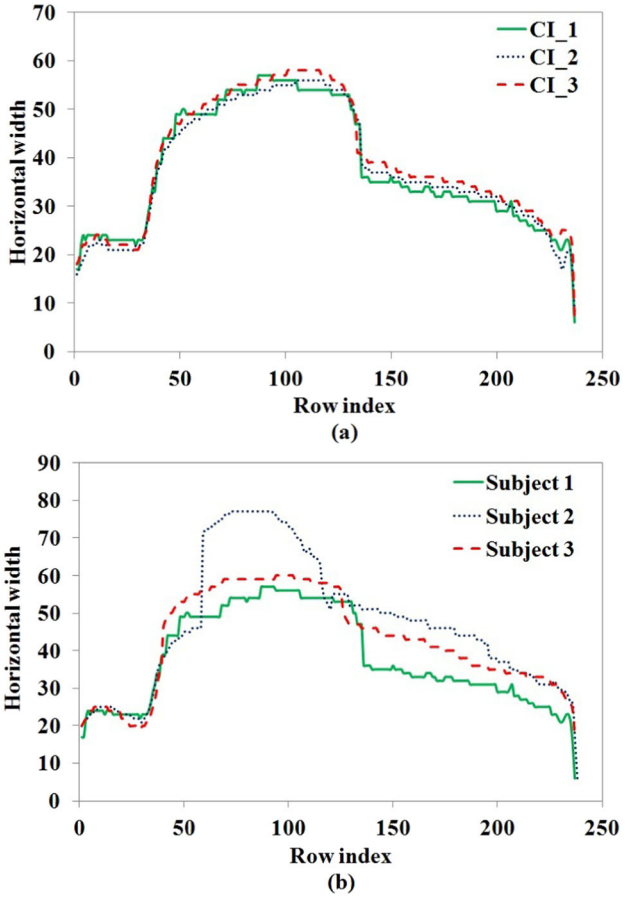

Fig. 3 Diagram showing the horizontal span vector obtained from **a** three contour images CI's belonging to the same subject and **b** a single contour image belonging to three different subjects

The separation of the curves represent a considerable difference between inter-class distances in Fig. 3b, 4b,and 5b. The discriminative power of the features under consideration is demonstrated by the small intra-class variances in Fig. 3a, 4a, and 5a. The shape of the CI's for the same subjects appears similar when observed in the feature space diagram. This ensures that the extracted characteristics are differentiating.

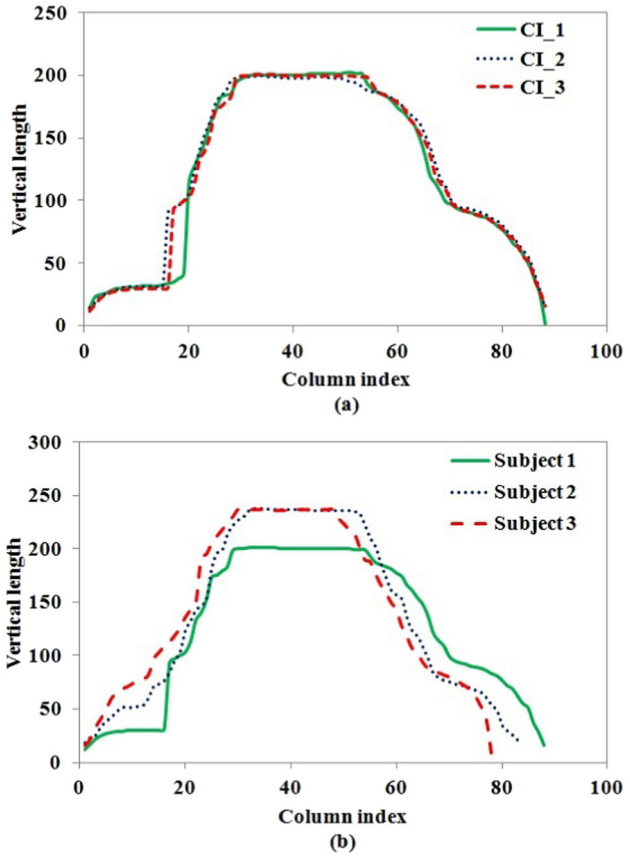

Fig. 4 Diagram showing the vertical span vector obtained from **a** three contour images CI's belonging to the same subject and **b** a single contour image belonging to three different subjects

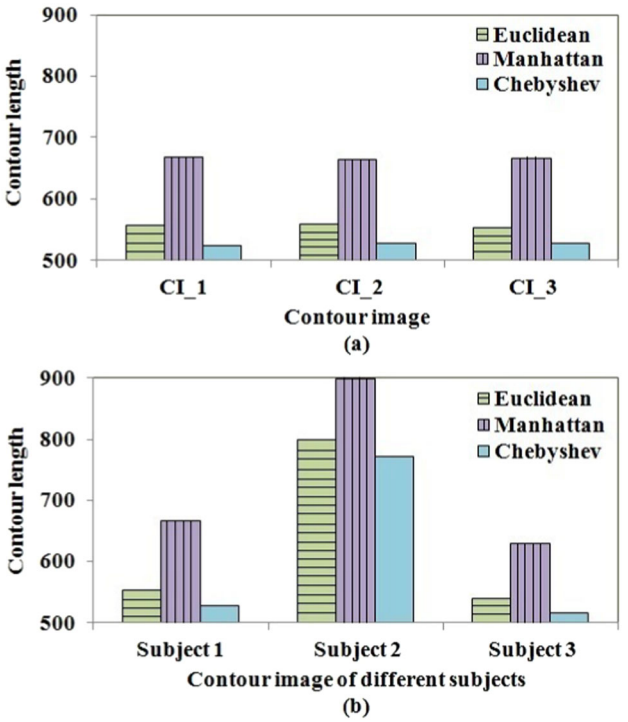

Fig. 5 Diagram showing the length contour vector obtained from **a** three contour images CI's belonging to the same subject and **b** a single contour image belonging to three different subjects

4 Experimental setup

In this study, the variations in spatial data cause discrepancies in the lengths of the region data vector found in each contour image. The range of values detected for different CI is consistently small, though it varies. Linear interpolation is employed to resample the vector and maintain consistent number of features for all CI's in the CASIA B gait dataset. Consequently, we determine and acquire the minimum and maximum length of the region data vector for all CI in the dataset. The minimum and maximum vector lengths are 298 and 315, respectively, with a 17-unit difference. The average length is 306.5. The size of the vector is adjusted to 307 through resampling. As a result, a feature vector of size 307 is generated for each contour image. The contour length vector does not change in size for any CI. Lastly, the formation of a vertex position vector of length 480 is achieved by extracting the arctangent of all contour vertices (left and right contour). To obtain a consistent feature vector from all subjects in a specific dataset, the same procedure is applied to CASIA A and CMU MoBo gait datasets.

This study is solely aimed to identify substantial features that contain maximum spatial information and are distinct for subjects, thereby enhancing performance. The nature of the computation of the proposed feature vectors ensures that all extracted measures in the feature set are positive scalar values.

The GEI and CI dimensions used in this study were 240x240 from CASIA A, CASIA B, and CMU MoBo dataset. Our analysis of the contour vertices and images from the training and testing datasets resulted in the creation of three feature vectors. Consequently, the ensemble classifier is used to classify the proposed gait features. In this case, we are dealing with a multiclass classification problem to predict the outcome. By utilizing the proposed feature vectors, the relevant sets of features are extracted and fed into a classification model to identify the subject. The prevailing research on gait recognition has focused on KNN, SVM, Random forest classifiers, which have yielded satisfactory prediction accuracy.

The literature investigates the use of multiple classifiers in gait recognition to tackle different challenges, and recent studies have demonstrated the effectiveness of ensemble classifiers in subject identification. Prediction is improved by utilizing an ensemble of classifiers that combine their opinions through majority or probability based voting. By leveraging the strengths of different classifiers, we can over-

Table 1 The proposed method's recognition accuracies on the CMU MoBo dataset are compared with existing methods

Method	B/F	F/B	B/I	F/I	B/S	F/S
Huang et al. [23]	88	92	88	84	96	96
Proposed method	**94**	**100**	**96**	**96**	**100**	**100**
Method	I/B	S/B	I/F	S/F	I/S	S/I
Huang et al. [23]	75	**96**	88	96	92	92
Proposed method	**92**	**98**	**94**	**100**	**100**	**98**

The bold value signifies the highest recognition accuracy obtained for a particular dataset

come their individual limitations. As a result, we investigated multiple advanced classifier techniques across various benchmark datasets and put forward a versatile prediction model. All categories of datasets can be processed using the proposed generalized model. By combining SVM, RF (bagging), and GBM (boosting), a single classification model is created, with all three classifiers working in parallel.

The output of the proposed ensemble classifier is determined by the highest probability-based voting, using probability values provided by each classifier for the given subjects. The highest average probability class determines the classification of the subject, which is obtained by averaging the output probabilities from the three classifiers. The SVM classifier was applied in this study with C=4.0 as the penalty parameter and the RBF kernel function, chosen for its superior performance in handling input noise. It is a widely known fact that adding more decision trees in the RF classifier decreases over-fitting and enhances prediction accuracy. Consequently, a RF classifier is employed, consisting of 335 decision trees, a value determined through empirical identification.

We observed that adding more trees did not result in better prediction accuracy in our experiments. By selecting regression trees as weak predictors and negative gradient multinomial deviance as the loss function, we implemented the GBM classifier. Gradient boosting can handle over-fitting fairly well with a higher number of weak predictors (boosting stages). Consequently, we decided to set the number of boosting stages at 335. It should be mentioned that the hyperparameters of our ensemble classifier remain constant throughout all experiments, with the prediction accuracies documented across all datasets.

5 Experimental results and discussion

In this empirical study, we used three well-known gait datasets, namely CASIA A, CASIA B, and CMU MoBo, to evaluate the performance of the proposed feature extraction method. In the CASIA A gait dataset [24], there are 20

Table 2 The average recognition accuracy of the concatenated vector compared to three individual feature vectors

Database	View	Ver_v	L_C	RD_v	FV
CASIA A	0^0	91.11	83.56	95.21	**100.0**
CMU MoBo	I/F	77.00	62.00	83.00	95.00
CMU MoBo	I/S	85.00	70.00	84.00	93.00
CMU MoBo	I/B	81.00	73.00	84.00	93.00
CMU MoBo	B/S	89.00	80.00	95.00	100.0
CMU MoBo	B/F	79.00	65.00	85.00	95.00
CMU MoBo	B/I	71.00	68.00	87.00	97.00
CMU MoBo	S/B	83.00	74.00	92.00	99.00
CMU MoBo	S/F	93.00	76.00	93.00	100.0
CMU MoBo	S/I	85.00	75.00	94.00	99.00
CMU MoBo	F/S	89.00	78.00	92.00	100.0
CMU MoBo	F/I	85.00	72.00	86.00	97.00
CMU MoBo	F/B	88.00	79.00	94.00	100.0
CASIA B	0^0(NM/NM)	79.66	64.67	92.50	99.60
CASIA B	180^0(NM/NM)	80.77	68.06	90.98	99.10
CASIA B	0^0(NM/BG)	81.10	68.00	90.44	99.44
CASIA B	180^0(NM/BG)	76.42	56.00	89.47	98.97
CASIA B	0^0(NM/CL)	86.97	65.19	95.00	99.47
CASIA B	180^0(NM/CL)	84.06	56.23	91.76	99.22
Average		83.42	70.19	90.22	**98.55**

The bold value signifies the highest recognition accuracy obtained for a particular dataset

subjects. As a result, we acquired 80 gait sequences from 20 subjects at the 0^0 angle. Table 2 presents the results of the proposed approach on CASIA A dataset for 0^0 view. For training, three sequences are selected out of the four, leaving one for testing. According to the results presented in Table 2, the proposed method yielded a 100

In this work, the results from the CMU MoBo dataset are presented, which consists of gait videos capturing 25 individuals walking on a treadmill. The gait videos were recorded with different walking techniques: fast walk (F), slow walk (S), walking with a ball (B), and walking on an incline (I). For both the gallery and probe datasets, all four forms of walking (F/B representing gallery F and probe B) were employed.

The results of the proposed approach on CMU MoBo dataset for the frontal view is shown in Table 1. Table 1 provides clear evidence that the proposed method has achieved a high CCR in most cases and yielded compelling results. It demonstrated exceptional performance on the CMU MoBo dataset, surpassing other methods for almost all gallery/probe combinations. The experiment primarily examined difficult cases, including walking with a ball and on an inclined plane such as B/I, F/I, B/F, I/B, I/F, and F/B, apart from changes in walking speed like S/F and F/S. The performance of the proposed method was impressive, especially in the most challenging cases.

Table 3 On the CASIA B gait dataset, the recognition rates of the proposed method

Exp	Gallery set	Gallery size	Probe set	Probe size	CCR (%)
1	0^0(NM)	124 × 4	180^0(NM)	124 × 4	96.50
2	0^0(NM)	124 × 4	180^0(NM)	124 × 3	97.77
3	0^0(NM)	124 × 4	180^0(NM)	124 × 2	97.82
4	0^0(NM)	124 × 4	180^0(NM)	124 × 1	96.00
5	0^0(NM)	124 × 4	180^0(BG)	124 × 2	97.24
6	0^0(NM)	124 × 4	180^0(BG)	124 × 1	99.00
7	0^0(NM)	124 × 4	180^0(CL)	124 × 2	97.50
8	0^0(NM)	124 × 4	180^0(CL)	124 × 1	98.17
9	180^0(NM)	124 × 4	0^0(NM)	124 × 4	95.28
10	180^0(NM)	124 × 4	0^0(NM)	124 × 3	94.73
11	180^0(NM)	124 × 4	0^0(NM)	124 × 2	93.95
12	180^0(NM)	124 × 4	0^0(NM)	124 × 1	96.52
13	180^0(NM)	124 × 4	0^0(BG)	124 × 2	97.89
14	180^0(NM)	124 × 4	0^0(BG)	124 × 1	98.10
15	180^0(NM)	124 × 4	0^0(CL)	124 × 2	98.50
16	180^0(NM)	124 × 4	0^0(CL)	124 × 1	99.00

Table 4 Evaluating the performance of the proposed method and existing methods on CASIA B gait dataset

	0^0	180^0	0^0	180^0	0^0	180^0
Methodology	NM/NM	NM/NM	NM/BG	NM/BG	NM/CL	NM/CL
Alotaibi and Mahmood [25]	90.67	83.99	91.98	87.76	88.77	90.00
Choudhury and Tjahjadi [26]	100.0	99.00	93.00	89.00	67.00	66.00
Isaac et al. [27]	98.50	98.99	95.00	94.44	97.00	93.94
Rida et al. [28]	97.97	97.58	72.76	76.11	80.49	83.06
Anusha and Jaidhar [29]	98.70	98.97	98.56	95.06	97.56	94.58
Proposed method	**99.60**	**99.10**	**99.44**	**98.06**	**99.11**	**98.22**

The bold value signifies the highest recognition accuracy obtained for a particular dataset

Table 5 The proposed method's recognition accuracies on CASIA A and CASIA B gait dataset are compared to existing contour-based methods

	0^0 (NM)	0^0 (NM)
Method	CASIA B	CASIA A
Ye and Wen [30]	83.37	92.25
Wang et al. [31]	72.14	88.75
Anusha and Jaidhar [29]	98.70	97.00
Liu et al. [32]	98.99	**100.0**
Lee et al. [33]	97.39	97.75
Proposed method	**100.0**	**100.0**

The bold value signifies the highest recognition accuracy obtained for a particular dataset

We assessed the proposed method using the CASIA B gait dataset. This dataset contains gait information from 124 subjects, captured from 11 angles between 0^0 and 180^0. For each subject, there are six normal walking sequences (NM), two carrying conditions sequences (BG), and two clothing variations sequences (CL).

The dataset was subjected to two experiments. The training initially employed the first four NM sequences. In order to evaluate normal, clothing, and carrying variations, the other two sequences of NM, CL, and BG were employed for testing purposes. The proposed method was tested on both 0^0 and 180^0 views to determine its effectiveness, given the considerable resemblance in the GEI images. Our proposed method proved to be significantly better than other methods, as shown in Table 4. The results highlighted how well it could handle variations in carrying and clothing.

Secondly, we compiled a training dataset that included NM gait sequences from both 0^0 and 180^0 viewpoints. Each subject was assigned four NM gait sequences for the training process. The training dataset contained 496 different gait patterns. Table 3 displays the varying number of CI's in the testing dataset. Table 3 showcases the results of 16 experiments using the proposed method. Experimental results confirmed the effective capture of shape dynamics in frontal gait images by the proposed method. Table 2 displays the recognition accuracies for CASIA A, CASIA B, and CMU

MoBo datasets using each of the four feature vectors individually as well as in concatenation, denoted as feature vector FV. Observations showed that the feature vector FV exhibited greater distinguishability compared to the individual feature vectors. RD_v had the highest average CCR among the three feature vectors, while L_C had a lower average CCR. The use of feature vector FV resulted in an average recognition accuracy increase of 8.33%, surpassing the individual accuracies of the four feature types. Due to its susceptibility to shape variations in a gait sequence, the proposed feature vector demonstrated the highest recognition accuracy.

The performance of the proposed method is compared to other contour based gait recognition methods in Table 5. Statistical shape analysis serves as the basis for gait recognition in both the contour-based algorithms in Table 5 and the proposed method. This paper introduces an enhanced method for feature extraction. Its primary objective is to enhance the gaps between classes. The experimental findings in Table 5 demonstrate a significant improvement in performance for the proposed method over other contour-based methods discussed in the literature.

6 Conclusion

The study suggests an approach to extract features for improved frontal gait recognition performance. The gait features being proposed are captured from the contour image and its vertices. The key finding of this study is the identification of three feature vectors that are responsive to meaningful spatial alterations in gait sequences. Furthermore, the research also showcases how it affects the rise in inter-class variability. Experimental results demonstrate that using all three feature vectors together enhances gait recognition performance. The proposed features were proven effective through extensive experimentation on three gait databases. Based on the experimental results, it is evident that the proposed method surpasses several existing approaches discussed in the literature. Furthermore, future studies may focus on investigating more sophisticated classification tools to enhance gait recognition accuracy.

Acknowledgements The authors acknowledge the invaluable contributions of the CASIA [24] and CMU MoBo [34] teams in making the gait datasets available.

Author Contributions A.R - Conducted experiment and wrote the main manuscript. S.CK - Prepared figures and reviewed the manuscript.

Data Availability No datasets were generated or analysed during the current study.

Declarations

Conflict of interest The authors declare no conflict of interest.

References

1. Semwal, V.B., Raj, M., Nandi, G.C.: Biometric gait identification based on a multilayer perceptron. Robot. Auton. Syst. **65**, 65–75 (2015)
2. Anusha, R., Jaidhar, C.: Human gait recognition based on histogram of oriented gradients and haralick texture descriptor. Multimed. Tools Appl. **79**(11), 8213–8234 (2020)
3. Muramatsu, D., Makihara, Y., Yagi, Y.: View transformation model incorporating quality measures for cross-view gait recognition. IEEE Trans. Cybernet. **46**(7), 1602–1615 (2016)
4. Soriano, M., Araullo, A., Saloma, C.: Curve spreads-a biometric from front-view gait video. Pattern Recognit. Lett. **25**(14), 1595–1602 (2004)
5. Sivapalan, S., Chen, D., Denman, S., Sridharan, S., Fookes, C.: Gait energy volumes and frontal gait recognition using depth images. In: 2011 International Joint Conference on Biometrics (IJCB), IEEE, pp. 1–6 (2011)
6. Chattopadhyay, P., Sural, S., Mukherjee, J.: Frontal gait recognition from occluded scenes. Pattern Recognit. Lett. **63**, 9–15 (2015)
7. Chattopadhyay, P., Roy, A., Sural, S., Mukhopadhyay, J.: Pose depth volume extraction from rgb-d streams for frontal gait recognition. J. Vis. Commun. Image Represent. **25**(1), 53–63 (2014)
8. Chattopadhyay, P., Sural, S., Mukherjee, J.: Frontal gait recognition from incomplete sequences using rgb-d camera. IEEE Trans. Inf. Forensics Secur. **9**(11), 1843–1856 (2014)
9. Ryu, J., Kamata, Si.: Front view gait recognition using spherical space model with human point clouds. In: 2011 18th IEEE International Conference on Image Processing, IEEE, pp. 3209–3212 (2011)
10. Maity, S., Abdel-Mottaleb, M., Asfour, S.S.: Multimodal low resolution face and frontal gait recognition from surveillance video. Electronics **10**(9), 1013 (2021)
11. Deng, M., Fan, Z., Lin, P., Feng, X.: Human gait recognition based on frontal-view sequences using gait dynamics and deep learning. IEEE Trans. Multimed. **26**, 117–126 (2023)
12. Zhang, Z., Tran, L., Liu, F., Liu, X.: On learning disentangled representations for gait recognition. IEEE Trans. Pattern Anal. Mach. Intell. **44**(1), 345–360 (2020)
13. Deng, M., Zhong, Z., Zou, Y., Wang, Y., Wang, K., Liao, J.: Human gait recognition based on frontal-view walking sequences using multi-modal feature representations and learning. Neural Process. Lett. **56**(2), 133 (2024)
14. Sheshadri, M.G.H., Okade, M.: Kinect based frontal gait recognition using skeleton and depth derived features. In: 2020 National Conference on Communications (NCC), IEEE, pp. 1–5 (2020)
15. Deng, M., Zou, Y., Zhu, W., Xing, M., Huang, Y., Yang, J.: Frontal-view gait recognition using discriminative dynamics feature representations and learning. J. Electr. Imaging **33**(1), 013,025-013,025 (2024)
16. Isaac, E.R., Elias, S., Rajagopalan, S., Easwarakumar, K.: Trait of gait: A survey on gait biometrics. arXiv preprint arXiv:1903.10744 (2019)
17. Parashar, A., Shekhawat, R.S., Ding, W., Rida, I.: Intra-class variations with deep learning-based gait analysis: a comprehensive survey of covariates and methods. Neurocomputing **505**, 315–338 (2022)
18. Xu, D., Zhou, H., Quan, W., Jiang, X., Liang, M., Li, S., Ugbolue, U.C., Baker, J.S., Gusztav, F., Ma, X., et al.: A new method proposed for realizing human gait pattern recognition: inspirations for the application of sports and clinical gait analysis. Gait Posture **107**, 293–305 (2024)
19. Anusha, R., Jaidhar, C.: Speed-invariant gait recognition using correlation factor lists for classroom attendance systems. In: Inter-

national Conference on Machine Learning, Image Processing, Network Security and Data Sciences, Springer, pp. 281–290 (2023)
20. Rani, V., Kumar, M.: Human gait recognition: a systematic review. Multimed. Tools Appl. **82**(24), 37,003-37,037 (2023)
21. Maple, C.: Geometric design and space planning using the marching squares and marching cube algorithms. In: Proceedings. 2003 International Conference on Geometric Modeling and Graphics, IEEE, pp. 90–95 (2003)
22. Sayeed, F., Hanmandlu, M.: Properties of information sets and information processing with an application to face recognition. Knowl. Inf. Syst. **52**(2), 485–507 (2017)
23. Huang, C.C., Hsu, C.C., Liao, H.Y., Yang, S.H., Wang, L.L., Chen, S.Y.: Frontal gait recognition based on spatio-temporal interest points. J. Chin. Inst. Eng. **39**(8), 997–1002 (2016)
24. Zheng, S.: (Accessed 27 Jul 2017) CASIA Gait Database. URL http://www.sinobiometrics.com
25. Alotaibi, M., Mahmood, A.: Improved gait recognition based on specialized deep convolutional neural network. Comput. Vis. Image Underst. **164**, 103–110 (2017)
26. Choudhury, S.D., Tjahjadi, T.: Robust view-invariant multiscale gait recognition. Pattern Recognit. **48**(3), 798–811 (2015)
27. Isaac, E.R., Elias, S., Rajagopalan, S., Easwarakumar, K.: View-invariant gait recognition through genetic template segmentation. IEEE Signal Process. Lett. **24**(8), 1188–1192 (2017)
28. Rida, I., Jiang, X., Marcialis, G.L.: Human body part selection by group lasso of motion for model-free gait recognition. IEEE Signal Process. Lett. **23**(1), 154–158 (2016)
29. Anusha, R., Jaidhar, C.D.: Frontal gait recognition based on hierarchical centroid shape descriptor and similarity measurement. In: 2019 International Conference on Data Science and Engineering (ICDSE), IEEE, pp 71–76 (2019)
30. Ye, B., Wen, Y.: A new gait recognition method based on body contour. In: 2006 9th International Conference on Control, Automation, Robotics and Vision, IEEE, pp 1–6 (2006)
31. Wang, L., Ning, H., Hu, W., Tan, T.: Gait recognition based on procrustes shape analysis. In: Proceedings. International Conference on Image Processing, IEEE, vol 3, pp III–III (2002)
32. Liu, L., Yin, Y., Qin, W., Li, Y.: Gait recognition based on outermost contour. Int. J. Comput. Intell. Syst. **4**(5), 1090–1099 (2011)
33. Lee, C.P., Tan, A.W., Tan, S.C.: Gait recognition via optimally interpolated deformable contours. Pattern Recognit. Lett. **34**(6), 663–669 (2013)
34. Gross, R., Shi, J.: The cmu motion of body (mobo) database. Tech. Rep. CMU-RI-TR-01-18, Carnegie Mellon University, Pittsburgh, PA (2001)